IEEE Access
Multidisciplinary | Rapid Review | Open Access Journal

Received March 4, 2020, accepted April 3, 2020, date of publication April 13, 2020, date of current version April 30, 2020.

Digital Object Identifier 10.1109/ACCESS.2020.2987545

Load Balancing in Hybrid VLC and RF Networks Based on Blind Interference Alignment

AHMAD ADNAN-QIDAN, (Member, IEEE), MÁXIMO MORALES-CÉSPEDES, (Member, IEEE), AND ANA GARCÍA ARMADA, (Senior Member, IEEE)
Department of Signal Theory and Communications, Universidad Carlos III de Madrid, 28911 Leganés, Spain

Corresponding author: Ahmad Adnan-Qidan (ahmadq@tsc.uc3m.es)

This work was supported in part by the Spanish National Project TERESA-ADA under Grant TEC2017-90093-C3-2-R and Grant MINECO/AEI/FEDER, UE, and in part by the research project GEOVEOLUZ-CM-UC3M funded by the call Programa de apoyo a la realización de proyectos interdisciplinares de I+D para jóvenes investigadores de la Universidad Carlos III de Madrid 2019–2020 under the frame of the Convenio Plurianual Comunidad de Madrid, Universidad Carlos III de Madrid.

ABSTRACT Visible light communications (VLC) are proposed for increasing the spectral efficiency and the number of devices served in indoor environments, while providing illumination through light emitting diodes (LED). For VLC, each optical access point (AP) provides a small and confined area of coverage. Since several sources of light are usually deployed in overlapping fashion in order to provide satisfactory illumination, VLC are limited by inter-cell interference. Moreover, transmission from a specific optical AP can be blocked by the elements of the scenario. On the other hand, radio-frequency (RF) systems such as WiFi are usually available in most of the indoor scenarios. In this work, we first propose a dynamic cell formation method for grouping the optical APs in multiple optical cells that cover a footprint each minimizing the inter-cell interference. After that, we use transmission based on blind interference alignment (BIA) in each optical cell. Considering the coexistence with RF systems based on orthogonal frequency division multiplexing (OFDM), a load balancing algorithm is proposed for managing the resources of the resulting hybrid VLC/RF network and determining the user association to each system. However, the complexity of this optimization problem is excessively high for practical VLC/RF networks. In order to obtain a suboptimal but tractable solution, we propose a decentralized optimization method based on Lagrangian multipliers. Simulation results show that the proposed scheme outperforms other approaches for user grouping and managing the resources of hybrid VLC/RF networks.

INDEX TERMS Visible light communications, blind interference alignment, user-centric, hybrid network, load balancing.

I. INTRODUCTION

The continuous demand on wireless data traffic makes the use of new spectrum beyond the tradicional radio-frequency (RF) bands a requirement for providing high data rates while supporting an exponentially increasing number of users [1]. Visible light communications (VLC) have become a promising technology for moving part of the indoor data traffic to the optical domain. Besides, VLC provide several advantages such as an enormous and unregulated bandwidth, avoiding the interference with RF systems, better security in the physical layer, high energy efficiency and a low-cost implementation [2], [3]. Each optical transmitter based on light emitting diode (LED) technology can be treated as an access point (AP) providing a small and confined area of coverage. Since multiple APs are deployed in a room to ensure satisfactory illumination, VLC systems are subject to interference that requires to be managed in order to achieve high data rates [4].

Transmission from several optical APs naturally configures a multiple-input multiple-output (MIMO) system. In this sense, transmit precoding (TPC) schemes such as zero-forcing (ZF) [5] or interference alignment (IA) [6] have been proposed for maximizing the degrees of freedom (DoF), i.e., the multiplexing gain, in RF systems. Beyond the need for channel state information at the transmitter (CSIT), the implementation of TPC schemes for VLC does not result straightforward. First, the transmitted signal of each optical

The associate editor coordinating the review of this manuscript and approving it for publication was Tachun Lin.

AP must be a non-negative real value once the precoding is applied. Typically, adding a DC-bias current is considered to solve this issue. However, out of the linear range of the LED transmitters, this constraint can lead to signal distortion [7]. Secondly, TPC schemes require coordination among the APs, which requires to deploy backhaul links supporting high-data rates. Although power line communications or dedicated fiber-optic links can be considered [4], they are challenging to implement while increasing the costs of the VLC systems. Moreover, the user-rate achieved by TPC schemes is subject to obtaining uncorrelated channel responses among the users. Notice that the lack of small scale effects in VLC increases the probability of correlation among the channel responses, which may lead to low data rates. The use of TPC schemes for VLC is proposed in several works such as [7]–[9].

In this context, we focus on a transmission scheme referred to as blind interference alignment (BIA) that provides a growth of DoF without the need for CSIT as the number of users increases [10]. BIA is based on exploiting the correlation among the channel variations of the users. Initially, BIA was proposed for RF systems using reconfigurable antennas at the receiver side [11]. Each reconfigurable antenna provides a set of linearly independent channel responses connected to single signal processing chain [12]. In [13], a reconfigurable photodetector is proposed for allowing the implementation of BIA in VLC. It is shown that BIA outperforms the rate achieved by TPC schemes in VLC scenarios. Moreover, there exist several features of BIA that motivate its implementation. In the following, we summarize the benefits of BIA in VLC systems

1) No CSIT is required for achieving a growth of DoF as the number of users increases. Applied to VLC, this fact reduces the use of uplink since the channel estimated by each user is not fed back to the optical APs. Notice that uplink transmission typically results challenging in VLC, which must be implemented through infrared (IR) communications or alternative RF systems such as WiFi or femtocells [3].
2) The BIA schemes are based on precoding matrices composed of zero and one values. Thus, in contrast to TPC schemes, BIA easily guarantees a non-negative and real transmitted signal, which inherently satisfies the constraints of the optical channel.
3) Cooperation among transmitters is not required to exchange the information to the users. Applied to VLC, this fact means that backhaul links supporting high-data rates among the optical APs are not required to be deployed. As a consequence, the complexity of the VLC network is reduced considerably.
4) In contrast to TPC schemes, the correlation among the channel responses of the users does not affect the achievable rate of each user.
5) The fabrication of reconfigurable photodetectors is less complex and much cheaper than for reconfigurable antennas [14].

However, BIA suffers a noise enhancement proportional to the number of users, which leads to a signal to noise ratio (SNR) degradation. Moreover, the required coherence time of the channel grows exponentially with the number of transmitters. As a consequence, alternative BIA schemes are required in order to manage a network composed of several APs as usually occurs in VLC.

The VLC systems are usually deployed in indoor scenarios where a complementary RF network is already available, e.g., WiFi or femtocells [15]. As a consequence, both technologies comprising the conventional RF and optical spectrum each converge to create a VLC/RF hybrid network [16]. In [17], these networks are proposed for improving the probability of blocking of the users. That is, the users that obtain a poor performance from the VLC system because they are blocked by any element of the scenario proceed to handover to the RF system. In such a way, the load balancing algorithm that maximizes the average user-rate in VLC/RF hybrid networks is proposed in [18]. However, transmission based on orthogonal frequency division multiplexing (OFDM) is considered in both systems. Specifically, an orthogonal resource management is considered so that transmission in each pair transmitter-receiver occurs in distinct time and frequency. This approach does not exploit the particular topology of the VLC systems composed of multiple APs that provide a small and confined area of coverage each, which allow us to reuse the transmission resource, either time or frequency. Exploiting the topology of the network in absence of CSIT in order to maximize the DoF through index coding, which in fact can be considered as a form of interference alignment, is proposed in [19].

At this point, we can briefly review the key ingredients that determine the performance of the hybrid VLC/RF networks. First, a user-centric approach is required in VLC systems by generating optical cells composed of several APs due to their small and confined area of coverage [20], [21]. Secondly, an efficient management of the network resources requires to consider the cell association to each user. The optimization of the network resources in small cell networks has been widely studied in [22], [23] considering a centralized solution. In [24], [25], the authors propose a decentralized solution for the resource management in heterogeneous networks. Third, the introduction of two technologies such as VLC and RF systems allows the load balancing for maximizing the performance of each user [26], [27]. These ingredients, i.e., user-centric cell formation, management of the network resources and load balancing are related among them and determine the performance in hybrid VLC/RF networks.

In this work, we consider a hybrid VLC/RF network taking into consideration the ingredients described above. Motivated by [19], we consider a topological approach in which the optical APs are grouped in elastic cells from a user-centric perspective. For this approach, we assume that transmission in the VLC system employs the BIA scheme while the RF system is based on OFDM. The main contributions of this work are

1) We derive a dynamic cell formation for hybrid VLC/RF networks based on a user-centric approach. For the VLC system, the use of BIA involves some limitations given by the number of users and optical APs that compose each optical cell. The proposed algorithm generates elastic cells that minimize the interference among them, also called inter-cell interference (ICI), while satisfying the constraints of noise enhancement and coherence time for BIA transmission.
2) Once the VLC network is divided into optical cells from the user-centric perspective, we formulate the load balancing optimization problem taking into consideration the resource management and the constraints of the hybrid VLC/RF network.
3) Solving the proposed load balancing algorithm through a centralized exhaustive search involves an excessively high complexity. We propose a decentralized solution based on Lagrangian multipliers that performs close to the optimal with a much lower complexity.

Simulation results show that the proposed dynamic cell formation outperforms other schemes such as assuming full connectivity between optical APs and users or dividing the network into static cells with a fixed number of optical APs per cell. Besides, the proposed load balancing algorithm improves the achievable rate with respect to the benchmarking schemes.

The remainder of this paper is organized as follows. In Section II the system model for hybrid VLC/RF networks is described. In Section III we present a brief overview of BIA. We introduce the benchmark methodologies for cell formation in Section IV, after that, the proposed dynamic cell formation algorithm is derived. In Section V we formulate the load balancing problem deriving the centralized and decentralized solutions while analyzing their complexity. Section VI presents some simulation results where the performance of the proposed scheme is compared with other benchmarking schemes. Finally, Section VII provides concluding remarks.

Notation. The following notation is considered in this work. Bold upper case and lower case letters denote matrices and vectors, respectively, $\mathbf{I}_M$ and $\mathbf{0}_M$ denote the $M \times M$ identity and zero matrices, respectively, while $\mathbf{0}_{M,N}$ corresponds to the $M \times N$ zero matrix, $[\,]^T$ and $[\,]^H$ are the transpose and the hermitian transpose operators, respectively, $\mathbb{E}$ is the statistical expectation and col{} is the column operator that stacks the considered vectors in a column.

II. SYSTEM MODEL

We consider an indoor hybrid network composed of both VLC and RF systems transmitting to $\mathcal{K}$, $k = \{1, \ldots, K\}$, users as is shown in Fig. 1. The VLC system is composed of $\mathcal{L}$, $l = \{1, \ldots L\}$, optical APs. Each optical AP corresponds to a LED lamp, which is composed of several low-power LEDs in a chip-on-board packing. In contrast, the RF system considers a single AP that provides coverage in the whole scenario. Moreover, each user can switch between both systems according to a predefined strategy. All the optical APs transmit over the same frequency and time. As a consequence, the overlapping areas of coverage, i.e., the illuminated footprints, are subject to interference. The whole set of APs is connected to a central unit as is shown in Fig. 1. In this sense, the optical APs can be grouped forming optical cells serving to a set of users in order to manage the interference. We assume that both systems do not have CSIT nor data sharing or cooperation exist among the optical APs. The knowledge of the central unit is limited to the network topology and the coherence time. Therefore, the tasks of the central unit are exclusively limited to synchronization and management of the network resources. The optical channel remains quasi-static and it only varies because of the users movement. In this sense, the average movement of the users corresponds to a speed of 3 Km/h.

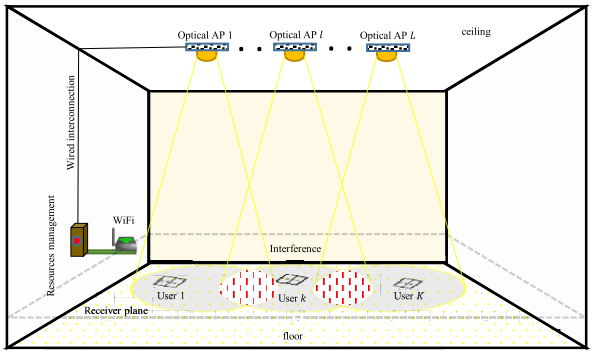

FIGURE 1. Diagram of an indoor hybrid VLC/WiFi network.

A. VLC SYSTEM

Each user is equipped with a reconfigurable photodetector as described in Fig. 2. The reconfigurable photodetector is equipped with M, $m = \{1, \ldots M\}$, photodiodes that provide linearly independent channel responses, each referred to as a preset mode, connected to a single signal processing chain through a selector. Moreover, each user selects a single preset mode at each time slot. The signal transmitted by the set of optical APs at time n is

$$\mathbf{x}[n] = \begin{bmatrix} x_1 & \ldots & x_L \end{bmatrix}^T \in \mathbb{R}_+^{L \times 1}, \tag{1}$$

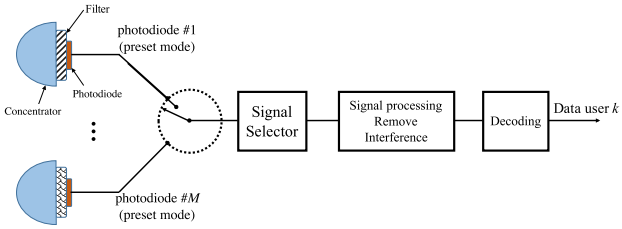

FIGURE 2. Architecture of the reconfigurable photodetector.

where x_l is the signal transmitted by the optical AP l. Thus, the signal received by user k corresponding to the preset mode m at time n is

$$y^{[k]}[n] = \mathbf{h}^{[k]}\left(m^{[k]}[n]\right)^T \mathbf{x}[n] + z^{[k]}[n], \tag{2}$$

where $\mathbf{h}^{[k]}(m^{[k]}[n]) \in \mathbb{R}_+^{L\times 1}$ is the channel vector between the L optical APs and user k for preset mode m selected at time n and $z^{[k]}[n]$ is real valued additive white Gaussian noise (AWGN) with zero mean and variance σ_z^2 [28].

According to [17], [18], the channel impulse in the frequency domain between transmitter l and user k for preset mode m, denoting f as the frequency, can be written as

$$h_l^{[k]}(m) = h_{l,\text{LoS}}^{[k]}(m) + h_{\text{diff}}(f)e^{-j2\pi f\,\Delta T}, \tag{3}$$

where $h_{l,\text{LoS}}^{[k]}(m)$ is the channel component given by the Line-of-Sight (LoS) contribution for preset mode m, h_{diff} is the diffuse component of the channel because of the reflection on walls, floor and ceiling and ΔT is the delay between both channel components.

The LoS component defined as DC gain is [28]

$$h_{l,\text{LoS}}^{[k]}(m) = \begin{cases} \dfrac{\gamma A}{d_{kl}^2} R_0(\phi_{kl}) g(\varphi_{kl}(m)) \cos^r(\varphi_{kl}(m)) & 0 \le \varphi_k \le \Psi_F \\ 0 & \text{if } \varphi_k \ge \Psi_F, \end{cases} \tag{4}$$

where γ and A denote the responsivity and the physical area of each photodiode, respectively, and d_{kl} is the distance between the optical AP l and user k. The irradiance and incidence angles from the optical AP l to the photodiode m of user k are denoted as ϕ_{kl} and $\varphi_{kl}(m)$,[1] respectively. For the photodiode m of user k, which provides the preset mode m, $g(\varphi_k(m))$ is the gain of the optical filter plus concentrator and r is the coefficient associated to its field-of-view (FOV) angle Ψ_F. Moreover, in (4), R_0 denotes the Lambertian radiation intensity $R_0 = \dfrac{\nu+1}{2\pi}\cos^\nu(\phi)$, where $\nu = \dfrac{-\ln 2}{\ln(\cos(\phi_{1/2}))}$ is the order of Lambertian emission and $\phi_{1/2}$ is the transmitter semi-angle.

The diffuse component in the frequency domain is defined as [29]

$$h_{\text{diff}}(f) = \frac{A}{A_r}\cdot\frac{\rho_1}{(1-\rho)\left(1+j\dfrac{f}{f_c}\right)}, \tag{5}$$

where ρ_1 is the reflectivity of the region initially illuminated by the LED lights, A_r is the area of the room surface, ρ is the average reflectivity of the walls, floor and ceiling and f_c is the cut-off frequency of the optical channel. It is worth mentioning that the diffuse component does not depend on the selected preset mode.

[1]The photodiodes of each user are allocated in a physical area much smaller than the distance between the optical AP l and user k. Therefore, the influence of the selected preset mode m can be considered negligible to determine the irradiance angle, i.e., $\phi_{kl}(m) \approx \phi_{kl}$.

For the reconfigurable photodetector of user k each photodiode m, which provides the m-th preset mode is characterized by its polar and azimuthal angles denoted as $\alpha^{[k,m]}$ and $\theta^{[k,m]}$, respectively. The orientation vector of the photodiode m of user k is given by

$$\hat{\mathbf{n}}^{[k]}(m) = \Big[\sin(\theta^{[k,m]})\cos(\alpha^{[k,m]}), \sin(\theta^{[k,m]})\sin(\alpha^{[k,m]}), \cos(\theta^{[k,m]})\Big]. \tag{6}$$

Thus, the irradiance and the incidence angles are determined by

$$\phi_{kl} = \arccos\left(\frac{\hat{\mathbf{n}}.\mathbf{v}_{kl}}{\|\hat{\mathbf{n}}\|\|\mathbf{v}_{kl}\|}\right) \tag{7}$$

$$\varphi_{kl}(m) = \arccos\left(\frac{\hat{\mathbf{n}}_k(m).\mathbf{v}_{kl}}{\|\hat{\mathbf{n}}_k(m)\|\|\mathbf{v}_{kl}\|}\right) \tag{8}$$

respectively, where $\hat{\mathbf{n}}$ is the normal orientation of optical APs, which are pointing perpendicularly to the floor, and $\mathbf{v}_{kl}$ is the vector from the optical AP l and user k. At this point, there exist several configurations for allocating the set of photodiodes of each user so that they provide linearly independent channel responses. For instance, the pyramidal or hemispherical arrangements proposed in [30] or the use of distinct lenses and filters for each photodiode [13].

B. RF SYSTEM

For the RF system, we assume a WiFi system in which the downlink operates in the frequency band of 2.4 GHz. Moreover, orthogonal resource allocation based on OFDM is proposed where the available bandwidth in the RF spectrum, which is denoted as B_{RF}, is divided into Q, $q = \{1,\ldots,Q\}$, subcarriers. Thus, the multi-user interference is managed by allocating sets of orthogonal slots in time and frequency.

The gain of the WiFi channel for the considered frequency band in indoor scenarios can be modeled as in [17]. That is,

$$G^{[k]} = \sqrt{10^{\frac{-\text{PL}(d)}{10}}}\,h_r \tag{9}$$

where $G^{[k]}$ is the frequency response of the channel between the WiFi AP and user k. Moreover, in (9), h_r follows a Rayleigh distribution with variance σ_r^2 equal to 2.46 dB [18] and PL(d) denotes the large-scale fading because of path losses given by

$$\text{PL}(d) = \text{PL}(d_0) + 10\,p_m\log_{10}\left(\frac{d}{d_0}\right) + X_\mu, \tag{10}$$

where PL(d_0) is the reference path loss at distance d_0, p_m is the path loss exponent and X_μ corresponds to the shadowing component. Following the model proposed in [31] for WiFi propagation, PL(d_0) is equal to 47.9 dB for a distance $d_0 = 1$ m, $p_m = 1.6$ and X_μ is modeled by a Gaussian distribution with zero mean and standard deviation equal to 1.8 dB.

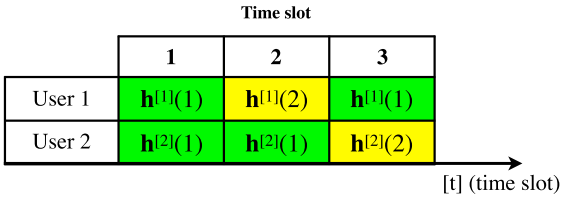

FIGURE 3. Pattern of switching preset modes of each user that compose the BIA supersymbol for $L = 2$ transmitters and $K = 2$ users. The channel response of user k at preset mode m is denoted as $\mathbf{h}^{[k]}(m)$.

III. BLIND INTERFERENCE ALIGNMENT

In this section, we present a brief overview of BIA scheme in order to introduce some useful notation [11], [13]. First, we describe a toy example in detail for illustrative purposes, after that, the general case is presented providing closed-form expressions of the achievable DoF and user-rate.

A. TOY EXAMPLE

Let us consider a VLC network composed of $L = 2$ optical APs and $K = 2$ users equipped with a reconfigurable photodetector capable of switching between two preset modes each. For this setting, both users follow a pattern of preset modes as described in Fig. 3. For instance, the user 1 switches from the first preset mode to the second preset mode in the time slot 2 and switches back to the first preset mode in the time slot 3. The pattern of preset modes for all the users is referred to as *supersymbol* from now on. It is worthy to recall that the optical channel must remain quasi-constant during the entire supersymbol so that the channel correlation between both users only depends on the selected preset mode. For the proposed supersymbol shown in Fig. 3, the transmitted signal is given by

$$\mathbf{x}_{\text{bia}} = \begin{bmatrix}\mathbf{x}[1]\\ \mathbf{x}[2]\\ \mathbf{x}[3]\end{bmatrix} = \begin{bmatrix}\mathbf{I}_2\\ \mathbf{I}_2\\ \mathbf{0}_2\end{bmatrix}\mathbf{u}^{[1]} + \begin{bmatrix}\mathbf{I}_2\\ \mathbf{0}_2\\ \mathbf{I}_2\end{bmatrix}\mathbf{u}^{[2]} \in \mathbb{C}^{6\times 1}, \quad (11)$$

where $\mathbf{x}[n] \in \mathbb{R}_+^{2\times 1}$ is the signal transmitted during time slot n and $\mathbf{u}^{[k]} = \begin{bmatrix}u_1^{[k]} & u_2^{[k]}\end{bmatrix}^T \in \mathbb{R}_+^{2\times 1}$ is the symbol sent to user k, where $u_l^{[k]}$ is the symbol transmitted from the optical AP l. Moreover, in (11), recall that $\mathbf{I}_2$ and $\mathbf{0}_2$ denote the 2×2 identity and all-zeros matrices, respectively. Notice that determining the transmitted signal does not requiere CSIT or data sharing. Then, focussing on user 1, the received signal is

$$\begin{bmatrix}y^{[1]}[1]\\ y^{[1]}[2]\\ y^{[1]}[3]\end{bmatrix} = \underbrace{\begin{bmatrix}\mathbf{h}^{[1]}(1)^T\\ \mathbf{h}^{[1]}(2)^T\\ \mathbf{0}_{2,1}{}^T\end{bmatrix}}_{\text{rank}=2}\mathbf{u}^{[1]} + \underbrace{\begin{bmatrix}\mathbf{h}^{[1]}(1)^T\\ \mathbf{0}_{2,1}{}^T\\ \mathbf{h}^{[1]}(1)^T\end{bmatrix}}_{\text{rank}=1}\mathbf{u}^{[2]} + \begin{bmatrix}z^{[1]}[1]\\ z^{[1]}[2]\\ z^{[1]}[3]\end{bmatrix}. \quad (12)$$

It can be easily seen that the interference is aligned in a rank-1 matrix while the desired symbol is contained in a rank-2 matrix. Hence, the interference due to transmission of $\mathbf{u}^{[2]}$ can be measured in the third time slot and subtracted afterwards. For user 1, the received signal after interference subtraction can be written as

$$\tilde{\mathbf{y}}^{[k]} = \underbrace{\begin{bmatrix}\mathbf{h}^{[1]}(1)^T\\ \mathbf{h}^{[1]}(2)^T\end{bmatrix}}_{\mathbf{H}^{[1]}}\mathbf{u}^{[1]} + \begin{bmatrix}z^{[1]}[1] - z^{[1]}[3]\\ z^{[1]}[2]\end{bmatrix}, \quad (13)$$

where $\tilde{\mathbf{y}}^{[k]} = \left[y^{[1]}[1] - y^{[1]}[3],\ y^{[1]}[2]\right]^T$. Notice that the matrix $\mathbf{H}^{[1]} = \left[\mathbf{h}^{[1]}(1)^T\ \mathbf{h}^{[1]}(2)^T\right]^T \in \mathbb{R}_+^{2\times 2}$ is a full rank matrix since it contains the 2 channel responses provided by 2 distinct preset modes of the reconfigurable photodetector. Therefore, the 2 DoF of $\mathbf{u}^{[1]}$ are decodable by solving (13) subject to noise distortion. Besides, notice that a noise enhancement occurs because of the interference subtraction. Similarly, using the signal received at time slots $\{1, 3\}$ and measuring the interference due to transmission of $\mathbf{u}^{[1]}$ at time slot 2, the user 2 can decode the 2 DoF contained in $\mathbf{u}^{[2]}$. Hence, each user achieves $\frac{2}{3}$ DoF per time slot. That is, the BIA scheme provides a sum-DoF equal to $\frac{4}{3}$ for the considered setting without CSIT nor data sharing among the optical APs. At this point, notice that orthogonal transmission schemes are limited to a sum-DoF equal to 1.

B. GENERAL CASE

Assuming that each user receives a useful signal from L transmitters, the BIA scheme is based on generating a supersymbol and a transmission structure that satisfy the following criterion; *the channel state of user k varies among L preset modes during the transmission of the intended symbol while the channel state of all other users $k' \neq k$ remains constant.* The time slots of user k that satisfy this criterion are referred to as an *alignment block* from now on.

For the general case, each alignment block of user k is composed of L time slots in which the reconfigurable photodetector of the user switches among L distinct preset modes, i.e., modifying the channel state. Thus, taking into consideration the BIA criterion described above, the supersymbol can be constructed recursively generating non-overlapping groups as described in Fig. 4. Therefore, for user k, the generic supersymbol contains $\ell = 1, \ldots, (L-1)^{K-1}$ alignment blocks, which carry L DoF each. That is, during the alignment block ℓ of user k the symbol $\mathbf{u}_\ell^{[k]} \in \mathbb{C}^{L\times 1}$ is transmitted. The first $L-1$ slots of each alignment block belong to Block 1, in which simultaneous transmission to the K users occurs. On the other hand, the last slot of each alignment block is allocated to Block 2 where each symbol is transmitted in orthogonal fashion. For the considered toy example, given by the supersymbol shown in Fig. 3 and the transmitted signal (11), the set of time slots $\{1, 2\}$ and $\{1, 3\}$ compose an alignment block for user 1 and user 2, respectively. Following the iterative construction of the supersymbol described in [11], the length of the supersymbol comprises

$$\Lambda_{\text{BIA}} = (L-1)^K + K(L-1)^{K-1}, \quad (14)$$

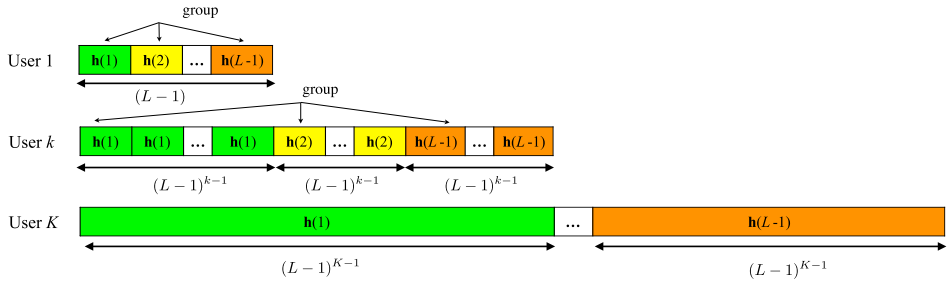

FIGURE 4. Recursively construction of Block 1 of the supersymbol for L transmitters and K users. Each color represents a preset mode.

time slots. Since each of the K users achieves L DoF in each of the $(L-1)^{K-1}$ alignment blocks, which are distributed over a supersymbol comprising Λ_{BIA} time slots, each user obtains $\text{DoF}_{\text{user}} = \frac{L}{L+K-1}$. Hence, the sum-DoF per time slot achieved by the K users is

$$\text{DoF}_{\text{BIA}} = K\,\text{DoF}_{\text{user}} = \frac{LK(L-1)^{K-1}}{\Lambda_{\text{BIA}}} = \frac{LK}{L+K-1}. \tag{15}$$

C. ACHIEVABLE USER-RATES OF BIA

Simultaneous transmission takes place during Block 1. Hence, the signal received during the first $L-1$ slots of the alignment block ℓ of user k are subject to interference because of transmission to all other users $k' \neq k$. Based on the BIA approach, the interference because of transmission to all other users $k' \neq k$ can be measured in the corresponding time slot of Block 2 and subtracted afterwards. The signal received by user k for the alignment block ℓ after interference subtraction can be written as

$$\tilde{\mathbf{y}}^{[k]} = \begin{bmatrix} \mathbf{h}^{[k]}(1)^T \\ \vdots \\ \mathbf{h}^{[k]}(L-1)^T \\ \mathbf{h}^{[k]}(L)^T \end{bmatrix} \mathbf{u}_\ell^{[k]} + \begin{bmatrix} z^{[k]}[1] - \sum_{k'\neq k}^{K} z^{[k]}[\tau] \\ \vdots \\ z^{[k]}[L-1] - \sum_{k'\neq k}^{K} z^{[k]}[\tau] \\ z^{[k]}[L] \end{bmatrix}, \tag{16}$$

where $\tilde{\mathbf{y}}^{[k]} \in \mathbb{R}_+^{L\times 1}$. Notice that, in (16), the temporal index refers to the position in the alignment block instead of the corresponding temporal index within the supersymbol, for the sake of simplicity, and τ is the time slot where the corresponding term of interference is measured. Assuming uniform resource allocation, each user obtains $(L-1)^{K-1}$ alignment blocks during the entire supersymbol. The ratio between the number of alignment blocks per user and the supersymbol length is denoted as B_k, which is equal to $\frac{1}{L+K-1}$ for uniform resource allocation. However, non-uniform allocation of the number of alignment blocks per user is possible following [32]. Therefore, the achievable rate of user k can be written as

$$R^{[k]} = B_k \mathbb{E}\left[\log_2 \det\left(\mathbf{I}_L + P_{\text{str}} \mathbf{H}^{[k]} \mathbf{H}^{[k]H} \mathbf{R}_z^{-1}\right)\right], \tag{17}$$

where P_{str} is the power allocated to the data stream given by the alignment block of the symbol $\mathbf{u}_\ell^{[k]}$,

$$\mathbf{H}^{[k]} = \left[\mathbf{h}^{[k]}(1)^T \ \ldots \ \mathbf{h}^{[k]}(L)^T\right]^T \in \mathbb{C}^{L\times L} \tag{18}$$

is the channel matrix of user k, which is a full-rank matrix, and

$$\mathbf{R}_z = \begin{bmatrix} K\mathbf{I}_{L-1} & \mathbf{0}_{L-1,1} \\ \mathbf{0}_{1,L-1} & 1 \end{bmatrix} \tag{19}$$

is the noise covariance matrix.

At this point, it is interesting to remark the following points; *i)* the supersymbol length grows as the number of optical APs and users increases (see (14)), which determine the channel coherence requirement, *ii)* a noise enhancement (see (19)) occurs as the number of users increases, *iii)* the BIA scheme described above assumes connectivity to all the L optical APs of the VLC system. As a consequence, alternative BIA schemes are required to overcome these issues as the number of users and/or transmitters increases.

D. APPLICATION TO VLC AND COSTS OF PROVIDING CHANNEL STATE INFORMATION

Typically, several optical APs are deployed in VLC scenarios. In order to manage the interference, the optical APs can be grouped to form an optical cell. Let us consider an optical cell comprising L optical APs transmitting to K users. Assuming CSIT, the achievable DoF is equal to $\min(L, K)$. Thus, applying BIA in the considered optical cell cancels the interference because of transmission to the K users of the cell while providing a DoF gain given by (15) without the need for CSIT [13]. Indeed, the DoF provided by BIA corresponds to the upper bound in absence of CSIT as demonstrated in [33]. However, interference among them, i.e., ICI, may appear from neighbouring optical cells. As described in the following section, forming optical cells requieres an user-centric perspective due to the small and confined area of coverage of each optical cell. In the following, we consider that BIA is implemented in each optical cell in order to cancel the multi-user interference while the ICI is managed by forming dynamic cells from a user-centric perspective.

The costs of providing CSI depends on the size of the optical cell, i.e., the number of optical APs that form the cell and

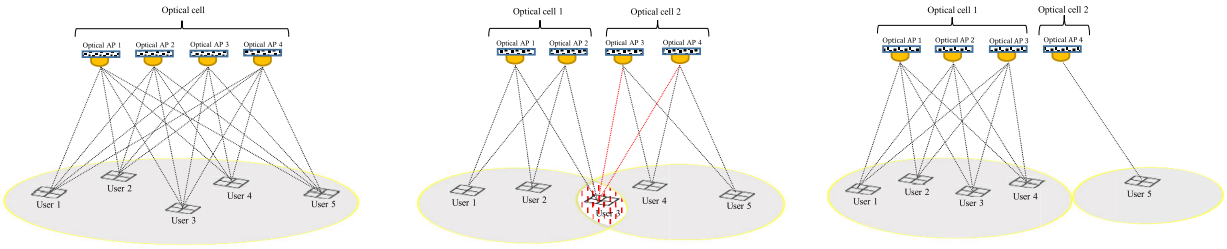

(a) (b) (c)

FIGURE 5. Cell formation methodologies for a specific network. (a) Full connectivity cell formation. (b) Static cell formation. (c) Dynamic cell formation.

the number of users served by them. In order to properly compare the performance of BIA with the TPC schemes, the costs of providing CSI must be considered [34]. In a frequency division duplex (FDD) system[2] providing CSIT involves first to transmit downlink estimation pilots (EP) in orthogonal fashion to estimate the channel contribution of each optical AP. After that, each user estimates the channel and feeds it back through the uplink. Once the precoding matrices for transmission to each user are calculated, transmission of pilots for detection is considered. The fraction of downlink transmission resources for pilot estimation and coherent detection are denoted as θ_{ep} and θ_{cd}, respectively. Besides, the fraction of transmission resources that are assigned to the uplink for feedback is denoted as θ_{fb}.

Let us consider a system comprising L transmitters serving K users. For TPC schemes, L orthogonal estimation pilots are transmitted in L dedicated time slots. The feedback of the estimated channel is proportional to the size of the channel vector, i.e., L components per user. Moreover, the overhead for coherent detection is proportional to the number of users. However, BIA schemes do not require CSIT, and therefore, estimation pilots and feedback of the estimated channel are not required, i.e., $\theta_{\text{ep}} = \theta_{\text{fb}} = 0$. On the other hand, the overhead for coherent detection is proportional to the number of preset modes employed in the BIA scheme. The costs of providing CSI for TPC and BIA schemes are listened in table. 1. For instance, the efficiency of the user-rate for TPC schemes taking into consideration the costs of providing CSIT is $\eta_{\text{tpc}} = 1-\left(L\left(\theta_{\text{ep}}+\theta_{\text{ep}}\right)+K\theta_{\text{cd}}\right)$. Similarly, the efficiency of the user-rate for BIA schemes is $\eta_{\text{bia}} = 1-LK\theta_{\text{cd}}$.

IV. OPTICAL CELL FORMATION

In this section, we first present two traditional cell formation methods as benchmarking schemes. After that, we derive a dynamic cell formation algorithm based on a user-centric perspective with the aim of satisfying the limitations of BIA in VLC.

[2]Notice that VLC are typically FDD since the uplink is usually implemented outside of the visible spectrum.

TABLE 1. Costs of providing CSI.

Type	Transmit precoding	BIA
Estimation pilots	$L\theta_{\text{csi}}$	0
Feedback	$L\theta_{\text{fb}}$	0
Coherent detection	$K\theta_{\text{cd}}$	$L\theta_{\text{cd}}$

A. FULL CONNECTIVITY CELL FORMATION

Typically, VLC systems consider a large number of optical APs to ensure satisfactory illumination. As a consequence, the coverage footprint of each optical AP overlaps with the area illuminated by other optical APs. The straightforward way of applying BIA in VLC systems consists on considering the whole set of optical APs as a single optical cell. This approach does not generate ICI and the multi-user interference is completely avoided. Notice that full connectivity between all the optical APs and each user is assumed for this approach. However, each optical AP provides connectivity within a small confined area of coverage. Moreover, transmission from an optical AP to a specific user can be blocked due to the elements of the scenario. As a consequence, the resulting channel matrix of this user (see (18)) may contain one or more columns with all values equal to zero, and therefore, it is a rank deficient matrix. Under this situation, the L DoF contained in each alignment block of the considered user are not decodable. In other words, full connectivity cannot be ensured for VLC systems, which leads to a DoF loss in comparison with (15) when applying BIA. Furthermore, this full connectivity approach can lead to extremely large supersymbols and a considerable SNR degradation because of the noise enhancement given by the interference subtraction, see (14) and (19), respectively.

For illustrative purposes, let us consider the network shown in Fig. 5(a) composed of $L = 4$ APs transmitting to $K = 5$ users. First, notice that the users located in the center of the scenario receive a useful signal from the whole set of APs, i.e., they achieve $\frac{4}{4+5-1} = \frac{1}{2}$ DoF each. In contrast, the users in each of the corners cannot receive a strong signal from the APs located in the apposite corner. As a

consequence, these users are limited to $\frac{3}{4+5-1} = \frac{3}{8}$ DoF. In this case, the full connectivity approach generates a supersymbol comprising $3^5 + 5 \times 3^4 = 648$ time slots that potentially achieves $\frac{20}{8} = 2.5$ DoF. However, the achievable DoF are $3 \times \frac{1}{2} + 2 \times \frac{3}{8} = \frac{18}{8} = 2.25$ DoF due to the lack of connectivity. Moreover, each user must subtract 4 terms of interference, which generate a noise enhancement penalizing the achievable rate (see (19)).

B. STATIC CELL FORMATION

In order to obtain a trade-off among the network connectivity, the length of the BIA supersymbol and the SNR degradation, the optical APs can be grouped forming a static deployment of optical cells. The L optical APs are grouped forming C, $c = \{1, \ldots, C\}$, uniform optical cells comprising $L_c = \frac{L}{C}$ neighbouring optical APs each.[3] For instance, $C = 2$ optical cells composed of 2 optical APs each are considered in the network proposed in Fig. 5(b). The network is divided into 2 cells comprising 2 optical APs each serving 2 and 3 users, respectively. Ignoring the ICI, this cell formation methodology could potentially achieve $\frac{6}{4} + \frac{4}{3} = 2.8$ DoF. It is worthy to notice that static cell formation could theoretically provide higher DoF than full connectivity approach for the considered scenario. This fact highlights the importance of adapting the cell formation to the topology of the network.

Once the optical cells have been defined, assuming transmission over the same transmission resource time and frequency, ICI may appear at the cell edges. For instance, the user in the center of the network shown in Fig. 5(b) is subject to ICI, and therefore, the achieved rate is considerably penalized. Moreover, according to the definition of DoF, this user obtains zero-DoF. As a consequence, the achievable DoF is reduced to $\frac{4}{3} + \frac{4}{3} = \frac{8}{3}$, i.e., $\frac{1}{6}$ below the DoF that can be potentially achieved ignoring the ICI. For traditional cellular networks, frequency reuse is typically proposed to mitigate the ICI. That is, adjacent cells transmit in different bandwidths. However, beyond the fact that the available bandwidth is split, for VLC networks this approach leads to a handover every few meters, which results unpractical for realistic implementations.

Discussion 1: The full connectivity approach allows us to completely cancel the interference while the achievable DoF is affected by the lack of connectivity. Besides, the extremely large supersymbol length and the noise enhancement hampers its implementation in a practical VLC system. On the other hand, forming static optical cells improves the achievable rates and relaxes the requirements of supersymbol length and noise enhancement. However, ICI may appear decreasing the achievable rate of the users. Moreover, this approach leads to a rigid user assignment to each cell. For VLC both approaches result unsuitable because of the small area of coverage of the optical APs. In the following, we propose a dynamic cell formation method based on the network topology, i.e., considering the position of the optical APs and also the distribution of the users. Thus, the cell formation minimizes the ICI while considering the limitation of supersymbol length and noise increase for implementing BIA in each optical cell.

[3] If $\frac{L}{C}$ is not an integer, the first $c = \{1, \ldots, \mathrm{mod}(L, C)\}$ cells contain $\lceil \frac{L}{C} \rceil$ optical APs while the last $c = \{\mathrm{mod}(L, C) + 1, \ldots, C\}$ cells are composed of $\lfloor \frac{L}{C} \rfloor$ optical APs.

C. DYNAMIC CELL FORMATION

Let us denote $\mathcal{V}_{\mathcal{L}_c}$ and $\mathcal{V}_{\mathcal{K}_c}$ as the sets of transmitters and users that compose the optical cell c, respectively. Notice that, in contrast to the previous approaches, each cell is given by the set of transmitters and also by the set of users assigned to that cell. Thus, cell c is defined as $\mathcal{C}_c = \mathcal{V}_{\mathcal{L}_c} \cup \mathcal{V}_{\mathcal{K}_c}$. Moreover, we consider that the transmitters and the users of the same cell cannot overlap, i.e., $\mathcal{V}_{\mathcal{L}_c} \cap \mathcal{V}_{\mathcal{L}_{c'}} = \emptyset$ and $\mathcal{V}_{\mathcal{K}_c} \cap \mathcal{V}_{\mathcal{K}_{c'}} = \emptyset$. That is, each optical AP and each user can only belong to a specific optical cell. The proposed dynamic cell formation algorithm is given by the following steps.

1) DETERMINE THE CELL SIZE

First, the algorithm specifies the maximum number of optical APs and users of each optical cell. These two parameters allow us to manage the constraints given by the supersymbol length and the noise enhancement of BIA. Denoting the number of optical APs and users for optical cell c as L_c and K_c, respectively, these two constraints are given by

$$(L_c - 1)^{K_c} + K_c(L_c - 1)^{K_c - 1} \leq \Lambda_{\max} \tag{20}$$

$$K_c \leq K_{\max}, \tag{21}$$

where $\Lambda_{\max}$ and $K_{\max}$ are the supersymbol length that satisfies the channel coherence requirement and the number of users that provides a SNR degradation for a target user-rate due to the noise enhancement, respectively.

2) DYNAMIC USER GROUPING

Once the maximum number of optical APs and users that can compose an optical cell has been defined, each optical cell is obtained dynamically according to the users distribution. The proposed grouping strategy is defined as follows.

1) Each optical AP l selects the closest user k, i.e.,

$$k = \arg\min_{k \in K} \mathrm{d}(l, k), \tag{22}$$

where $\mathrm{d}(l, k)$ denotes the Euclidean distance between optical AP l and user k. Thus, $\mathrm{d}(l, k) = \sqrt{(\check{x}_l - \check{x}_k)^2 + (\check{y}_l - \check{y}_k)^2}$ where $(\check{x}_l, \check{y}_l)$ and $(\check{x}_k, \check{y}_k)$ are the locations of optical AP l and user k, respectively.

2) The construction of a dynamic optical cell starts from a random pair given by the transmitter l and user k associated to this transmitter as described in the first step, which has not been chosen so far to form an optical cell c. We define the centroid of the optical cell l at the i-th iteration as $\zeta_c(i) = \left(\check{x}_{\zeta_c}(i), \check{y}_{\zeta_c}(i)\right)$. Notice that at the first iteration, the centroid $\zeta_c(i = 1)$ is given by the coordinates $(\check{x}_k, \check{y}_k)$ of user k. At this point, the

cell c is composed of $\mathcal{V}_{\mathcal{L}_c} = \{l\}$ and $\mathcal{V}_{\mathcal{K}_c} = \{k\}$ whose centroid is given by ζ_c.

3) The optical cell c is expanded by the merging with other pairs given by transmitter l' and user k' if and only if the users $\mathcal{V}_{\mathcal{K}_c} = \{k, k'\}$ receive a useful signal from the optical APs $\mathcal{V}_{\mathcal{L}_c} = \{l, l'\}$. That is, $\mathrm{d}\left(\forall l \in \mathcal{V}_{\mathcal{L}_c}, k'\right) \leq d_{th}$ and $\mathrm{d}\left(l', \forall k \in \mathcal{V}_{\mathcal{K}_c}\right) \leq d_{th}$, where d_{th} is the distance that delimits the footprint of each optical cell.[4] After that, the center of the optical cell c is updated to

$$\zeta_c(i) = \left(\frac{\check{x}_{\zeta_c}(i-1) + \check{x}_{k'}}{2}, \frac{\check{y}_{\zeta_c}(i-1) + \check{y}_{k'}}{2}\right). \quad (23)$$

Continue in the same fashion until there are not pairs transmitter-user that provide connectivity in the considered cell c, i.e, $\mathcal{V}_{\mathcal{L}_c}$ and $\mathcal{V}_{\mathcal{K}_c}$, or the cell size specified in (20) and (21) is reached. Notice that each optical cell is formed iteratively including the transmitter-user pairs that satisfy the conditions determined in this step while updating the centroid of the cell. This step determines the footprint of the optical cell c.

4) Once the optical APs that compose the optical cell c are determined, the algorithm considers the users that are not paired to any optical AP (see step 2) and can be served by the cell c. Thus, the set $\mathcal{V}_{\mathcal{K}_c}$ is updated with the users contained in the footprint of the cell c,

$$\mathcal{V}_{\mathcal{K}_c} = \mathcal{V}_{\mathcal{K}_c} \cup \{k \in \mathcal{K}, \mathrm{d}(\zeta_c(i), k) \leq d_{th}\}. \quad (24)$$

This step is constrained to the maximum number of users per cell $K_{\max}$. After that, the centroid of the optical cell c is updated by averaging the locations of new included users according to (23).

5) Go to the step 2) until the L optical APs are arranged in C dynamic cells. The users that are not assigned to any optical cell c are assigned to the RF system.

The steps that compose the proposed dynamic cell formation are summarized in the flowchart shown in Fig. 6. The optical cells are constructed dynamically as the distribution of the users changes. Therefore, the ICI is minimized in comparison with the static cell formation scheme. Considering the toy-example described in Fig. 5(c), 2 optical cells are obtained; the cell 1 comprising 3 optical APs serving 4 users and an optical cell composed of a single optical AP transmitting to a single user. Applying BIA in each cell, $2 + 1 = 3$ DoF are achieved for this case, which outperforms both the full connectivity and static cell formation approaches.

After applying the proposed cell formation scheme, the VLC/RF network is divided into C, $c = \{1, 2, \ldots, C\}$, optical cells each given by $\mathcal{V}_{\mathcal{L}_c} \cup \mathcal{V}_{\mathcal{K}_c}$. Moreover, the index $c = 0$ is reserved for the RF cell, which corresponds to the set of users $\mathcal{V}_{\mathcal{K}_0}$ that are assigned directly to the RF system. However, notice that some users of cell c can be blocked although they are located within the coverage footprint of the corresponding cell or they simply obtain a poor channel from the transmitters of the corresponding optical cell. For the optical network, the number of users has an impact on the SNR degradation because of the interference subtraction and on the number of alignment blocks per user, which determines the achievable DoF (see (15)). Similarly, the RF network divides the available bandwidth into subcarriers allocating a block of them to each user in orthogonal fashion. As a consequence, once the dynamic cell formation is performed, a load balancing algorithm is considered for managing the handover between the VLC and WiFi networks and allocating the transmission resources in hybrid VLC/RF networks.

[4]The footprint of each optical AP is given by the radiation semi-angle. Assuming that all the users are distributed over a plane with a distance h away from the ceiling, the footprint of each optical AP is $d_{th} = h \cdot \tan\left(\phi_{1/2}\right)$.

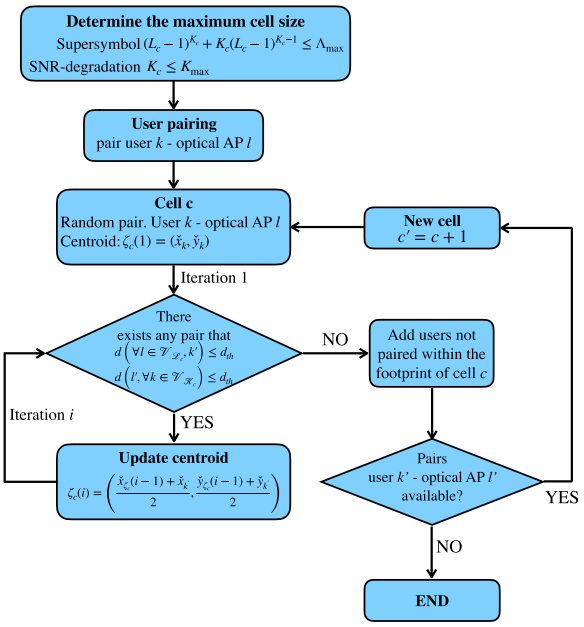

FIGURE 6. Flowchart of the dynamic cell formation algorithm.

V. LOAD BALANCING ALGORITHM

In this section, we derive a load balancing algorithm for hybrid VLC/RF networks. For homogeneous cellular networks, e.g., macrocell networks, the user assignment and resource management usually consider SNR maximization, referred to as max-SNR from now on. That is, each user is assigned to the cell from which the user receives the greatest SNR. However, for hybrid VLC/RF networks, both systems operate in different sections of the spectrum and the SNR varies considerably between both systems, which can lead to overloading one of them. In this sense, it is more suitable to consider the achievable user-rate as the variable to optimize instead of the SNR since it depends on both the SNR and the amount of resources allocated to that user. Moreover, recall that for BIA the resulting SNR depends on the number of users in each cell whose interference must be subtracted. This approach is referred to as max-Rate from now on.

First, we obtain the user-rate of each system, either optical or RF, taking into consideration the dynamic cell formation.

After that, we formulate the load balancing problem and analyze the user assignment for both max-SNR and max-Rate approaches. This optimization problem can be solved from a centralized solution through an exhaustive search. In order to reduce the complexity of this method, we propose a decentralized solution based on decoupling the load balancing problem.

A. ACHIEVABLE USER-RATE FOR HYBRID VLC/WIFI NETWORKS BASED ON DYNAMIC CELL FORMATION

1) VLC SYSTEM

The BIA scheme described in Section III is implemented independently in each optical cell, which comprises L_c and K_c optical APs and users organized in the sets $\mathcal{V}_{\mathcal{L}_c}$ and $\mathcal{V}_{\mathcal{K}_c}$, respectively. Since the optical APs are grouped in cells, remaining ICI may appear between neighbouring cells. In this sense, since the proposed cell formation is aimed at minimizing the ICI, it is treated as noise assuming that the signal received from interfering cells is much lower than the desired signal. Let us define the relative power from optical cell c' received at user k in cell c taking the reference from the received power of optical cell c as $\alpha_{c'}^{[k,c]}$, i.e., $\alpha_{c}^{[k,c]}=1$. Thus, the signal received by user k of cell c during an alignment block after interference subtraction can be written as

$$\tilde{\mathbf{y}}^{[k,c]}=\mathbf{H}^{[k,c]}\mathbf{u}_{\ell}^{[k,c]}+\sum_{c'=1,c'\neq c}^{C}\sqrt{\alpha_{c'}^{[k,c]}}\mathbf{H}^{[k,c']}\mathbf{x}_{\ell}^{[c']}+\tilde{\mathbf{z}}^{[k,c]}, \tag{25}$$

where $\tilde{\mathbf{y}}^{[k,c]}\in\mathbb{R}^{L_c\times 1}$ is the signal received during the L_c time slots of the considered alignment block ℓ after interfering subtraction and $\mathbf{x}_{\ell}^{[c']}$ is the signal transmitted by the neighbouring optical cell c' during the considered alignment block in which transmission of the symbol of interest $\mathbf{u}_{\ell}^{[k,c]}$ occurs. Moreover, in (25),

$$\mathbf{H}^{[k,c]}=\left[\mathbf{h}^{[k,c]}(1)\ \ldots\ \mathbf{h}^{[k,c]}(L_c)\right]\in\mathbb{R}_{+}^{L_c\times 1}, \tag{26}$$

is the channel matrix of user k that contains L_c linearly independent channel responses, i.e., $\mathbf{H}^{[k,c]}$ is a full rank matrix, and $\tilde{\mathbf{z}}^{[k,c]}$ is the noise after interference subtraction defined by the covariance matrix

$$\mathbf{R}_{\tilde{z}}=\begin{bmatrix}K_c\mathbf{I}_{L_c-1} & \mathbf{0}_{L_c-1,1}\\ \mathbf{0}_{1,L_c-1} & 1\end{bmatrix}. \tag{27}$$

Therefore, the rate achieved by user k in cell c can be written as

$$r_{\mathrm{VLC}}^{[k,c]}=e_{\mathrm{VLC}}^{[k,c]}\eta_{\mathrm{bia}}\times\mathbb{E}\left[\log_2\det\left(\mathbf{I}_L+P_{\mathrm{str}}\mathbf{H}^{[k,c]}\mathbf{H}^{[k,c]H}\mathbf{R}_{\mathrm{z_I}}^{[k,c]-1}\right)\right], \tag{28}$$

where $e_{\mathrm{VLC}}^{[k,c]}$ is the ratio between the number of alignment blocks allocated to user k in cell c and the length of the supersymbol, i.e., considering uniform resource allocation $e_{\mathrm{VLC}}^{[k,c]}=\frac{1}{L_c+K_c-1}$, η_{bia} denotes the efficiency of BIA taking into consideration the costs of providing CSI, which are limited to coherent detection, P_{str} is the power allocated to the data stream given by $\mathbf{u}_{\ell}^{[k,c]}$ and

$$\mathbf{R}_{\mathrm{z_I}}^{[k,c]}=\mathbf{R}_{\tilde{z}}+P_{\mathrm{str}}\sum_{c'=1,c'\neq c}^{C}\alpha_{c'}^{[k,c]}\mathbf{H}^{[k,c']}\mathbf{H}^{[k,c']H}, \tag{29}$$

is the covariance matrix of the noise plus interference due to transmission from other optical cells.

2) RF SYSTEM

We consider a WiFi AP transmitting an OFDM signal with Q subcarriers assigning a set of subcarriers to each user in orthogonal fashion, i.e., avoiding the multi-user interference. Since a single WiFi AP is deployed in the same scenario, i.e., there is not interference from other WiFi APs, the long-term[5] SNR for each subcarrier of user k is

$$\mathrm{SNR}^{[k]}=\frac{|G^{[k]}|^2\Delta P_q}{N_0\Delta B_q}, \tag{30}$$

where $G^{[k]}$ is the channel gain of user k, which according to (9), ΔP_q is the transmit power allocated to each subcarrier, ΔB_q is the modulation bandwidth of each subcarrier and N_0 is the noise power spectral density. It is assumed that the transmit power is allocated equally to each subcarrier. Since $Q^{[k,c]}$ subcarriers are allocated to user k in cell c, the achievable rate of user k connected to the WiFi system is

$$r_{\mathrm{WiFi}}^{[k,c]}=e_{\mathrm{RF}}^{[k,c]}\log_2\left(1+\mathrm{SNR}^{[k]}\right), \tag{31}$$

where $e_{\mathrm{RF}}=\frac{\Delta B_q}{B_{\mathrm{RF}}}Q^{[k,c]}$ is the ratio between the bandwidth allocated to user k in cell c and the available bandwidth B_{RF}.

B. PROBLEM FORMULATION

We define the set $\mathcal{C}_T=\{0,1,\ldots,C\}$ that contains all the cells in the hybrid network, where $c=0$ corresponds to the WiFi cell. In this context, we obtain a generic expression of the achievable user-rate for both VLC and WiFi systems in order to formulate the optimization problem. Specifically, checking (28) and (31), notice that the user-rate in any cell of $\mathcal{C}_T$ can be written in a generic form as

$$R^{[k,c]}=e^{[k,c]}r^{[k,c]}, \tag{32}$$

where $r^{[k,c]}$ is the spectral efficiency achievable by user k in cell c, either optical or RF, and $e^{[k,c]}$ denotes the fraction of resources that cell c allocates to user k

$$e^{[k,c]}=\begin{cases}\dfrac{1}{L_c+K_c-1} & \text{if VLC system}\\ \dfrac{\Delta B_q}{B_{\mathrm{RF}}}Q^{[k,c]} & \text{if WiFi system.}\end{cases} \tag{33}$$

By using this notation it is possible to manage the resource allocation of each cell according to the spectral efficiency of

[5]Recall that the RF channel is subject to Rayleigh fading generating short-term variations. However, in this work we consider the Shannon capacity as the achievable rate for long-term SNR.

the users. Notice that, $r^{[k,c]}$ can be easily obtained checking (28) and (31) for both VLC and WiFi systems, respectively. Specifically,

$$r^{[k,c]} = \begin{cases} \mathbb{E}\left[\log_2 \det\left(\mathbf{I}_L + P_{\text{str}}\mathbf{A}^{[k,c]}\right)\right] & \text{if VLC system} \\ \log_2\left(1 + \text{SNR}^{[k]}\right) & \text{if WiFi system,} \end{cases} \tag{34}$$

where $\mathbf{A}^{[k,c]} = \mathbf{H}^{[k,c]}\mathbf{H}^{[k,c]H}\mathbf{R}_{\mathbf{z}_l}^{[k,c]-1}$ (see (28)). Therefore, the achievable rate of a generic user k corresponds to

$$R^{[k]} = \sum_{c\in\mathcal{C}_T} x^{[k,c]} e^{[k,c]} r^{[k,c]}, \tag{35}$$

where the variable $x^{[k,c]}$ determines the cell association, which is $x^{[k,c]} = 1$ if user k is in cell c and $x^{[k,c]} = 0$, otherwise.

The proposed load balancing algorithm aims at optimizing the sum-rate within the footprint of cell c obtained after the dynamic cell formation, i.e., for the users belonging to the set $\mathcal{V}_{\mathcal{K}_c}$. Besides, we consider the use of a utility function so that the user-rate is transformed by a function $U = f\left(R^{[k]}\right)$. Specifically, we consider the logarithmic function, i.e., $U(x) = \log(x)$, which naturally achieves load balancing and some level of fairness among the users [35]. Therefore, the optimization problem may be formulated by maximizing the aggregate utility function. That is,

$$\begin{aligned} \max_{x,e} \; & \sum_{k\in\mathcal{V}_{\mathcal{K}_c}} \log\left(\sum_{c\in\mathcal{C}_T} x^{[k,c]} e^{[k,c]} r^{[k,c]}\right) \\ \text{s.t.} \quad & \sum_{c\in\mathcal{C}_T} x^{[k,c]} = 1 \qquad \forall k \in \mathcal{V}_{\mathcal{K}_c} \\ & \sum_{k\in\mathcal{V}_{\mathcal{K}_c}} e^{[k,c]} \leq 1 \qquad \forall c \in \mathcal{C}_T \\ & 0 \leq e^{[k,c]} \leq 1,\; x^{[k,c]} \in \{0,1\},\; \forall c \in \mathcal{C}_T, \forall k \in \mathcal{V}_{\mathcal{K}_c}. \end{aligned} \tag{36}$$

The first constraint in (36) guarantees that each user may either connect to an optical cell or the WiFi system, the second constraint guarantees that the portion of transmission resources employed for each optical cell or the WiFi system is less than 1. Moreover, the last constraint considers the feasible region of the optimization variables, where $x^{[k,c]}$ and $e^{[k,c]}$ are binary and real variables between 0 and 1, respectively.

Interestingly, the objective function (see (36)) depends on the achievable user-rate, which involves the SNR and also the resources available in the hybrid VLC/RF network, instead of simply considering the SNR. In Fig. 7, the load distribution is depicted considering max-SNR in the hybrid VLC/WiFi network. It can be easily seen that the WiFi system is overloaded. However, the achievable sum-rate of the network can be improved assigning more users to the VLC system. On the other hand, the percentage of users associated to each system according to the proposed max-Rate load balancing approach

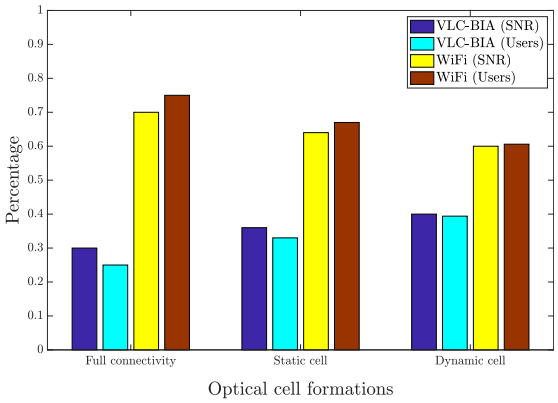

FIGURE 7. Max-SNR user association in hybrid VLC/WiFi considering different optical cell formation methods.

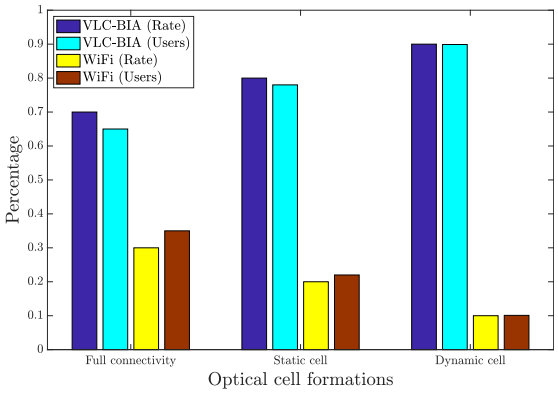

FIGURE 8. Max-rate user association in hybrid VLC/WiFi considering different optical cell formation methods.

is shown in Fig. 8. Notice that, the VLC system is serving a significant percentage of users, while the WiFi system serves an acceptable percentage of users. For the proposed dynamic cell formation approach, 90% of users are served by the VLC system while only 10% of them are connected to the WiFi. These results highlight the importance of employing a proper load balancing algorithm in hybrid VLC/RF networks.

C. CENTRALIZED SOLUTION

The optimization problem in (36) contains both a binary variable and a real positive variable that must be jointly solved. Thus, it is defined as a mixed integer non-linear programming problem. This problem is mathematically intractable since user association depends on the available resources and the resource allocation depends on the association of the users to either any optical cell or the WiFI system. In this sense, we adopt a restriction on variable $e^{[k,c]}$ by assuming uniform resource allocation [25]. Let us consider $\mathcal{V}_{\mathcal{K}_c}$ as a set of K_c users associated to optical cell c. Then, we define the load of cell c as $\sum_{k\in\mathcal{V}_{\mathcal{K}_c}} x^{[k,c]}$. Since BIA is implemented within each cell, $(L_c-1)^{K_c-1}$ alignment blocks are assigned to each user assuming uniform resource allocation. Thus, the assumption of $e^{[k,c]} = \dfrac{1}{K_c}$, means equal resources allocation among $K_c \times (L_c-1)^{K_c-1}$ alignments blocks over the supersymbol.

Therefore, according to the notation described above, the objective function of (36) becomes

$$f(x) = \sum_{k \in \mathcal{V}_{\mathcal{K}_c}} \log \left(\sum_{c \in \mathcal{C}_T} x^{[k,c]} \left(\frac{r^{[k,c]}}{\sum\limits_{k \in \mathcal{V}_{\mathcal{K}_c}} x^{[k,c]}} \right) \right). \quad (37)$$

Notice that, according to the first constraint in the optimization problem (36), i.e., $\sum_{c \in \mathcal{C}_T} x^{[k,c]} = 1$, user k must be associated with only one cell. Thus, the objective function (37) can be rewritten in equivalent form as

$$f(x) = \sum_{k \in \mathcal{V}_{\mathcal{K}_c}} \sum_{c \in \mathcal{C}_T} x^{[k,c]} \log \left(\frac{r^{[k,c]}}{\sum\limits_{k \in \mathcal{V}_{\mathcal{K}_c}} x^{[k,c]}} \right). \quad (38)$$

Consequently, the optimization problem (36) is modified to

$$\begin{aligned} &\max_{x} . f(x) \\ &\text{s.t.} \sum_{k \in \mathcal{V}_{\mathcal{K}_c}} x^{[k,c]} = K_c, \ \forall c \in \mathcal{C}_T \\ &\quad \sum_{c \in \mathcal{C}_T} x^{[k,c]} = 1, \ \forall k \in \mathcal{V}_{\mathcal{K}_c} \\ &\quad x^{[k,c]} \in \{0, 1\}, \forall c \in \mathcal{C}_T, \ \forall k \in \mathcal{V}_{\mathcal{K}_c}. \end{aligned} \quad (39)$$

This optimization problem obtains the resource management and user association that maximize the sum of the logarithmic utility function of the user-rate (see (36)). That is, it determines the number of users in each cell and the amount of transmission resources allocated to each user. Unfortunately, this centralized solution requires to share information among each of the optical cells and the WiFi AP in order to obtain a solution through an exhaustive search. As a consequence, the centralized solution is subject to a high computational complexity as the size of the network increases.

D. DECENTRALIZED SOLUTION

The complexity of the centralized solution can be excessively high for most of the network configurations. In the following, we propose a decentralized solution that reduces the complexity of the load balancing considerably. We formulate the load balancing algorithm given by solving the optimization problem (39) using the Lagrangian multiplier similarly as [27]. Thus, the optimization problem can be decoupled into two subproblems that can be solved separately. Specifically, the Lagrangian function is formulated as

$$f(x, k, \mu) = s(x, \mu_c) + g(k, \mu_c), \quad (40)$$

where

$$s(x, \mu_c) = \sum_{k \in \mathcal{V}_{\mathcal{K}_c}} \sum_{c \in \mathcal{C}_T} x^{[k,c]} \left(\log(r^{[k,c]}) - \mu_c \right), \quad (41)$$

and

$$g(k, \mu_c) = \sum_{c \in \mathcal{C}_T} K_c \left(\mu_c - \log(K_c) \right), \quad (42)$$

are two independent subproblems. The Lagrangian multiplier μ_c, $c \in \mathcal{C}_T$, corresponds to the constraint $\sum\limits_{c \in \mathcal{C}_T} x^{[k,c]} = 1$, $\forall k \in \mathcal{V}_{\mathcal{K}_c}$, described in (39). Thus, the solution of the optimization problem is determined by the function $f(x, k, \mu_c)$. That is,

$$\min_{\mu_c} . f(x, k, \mu_c). \quad (43)$$

The problem in (43) is dual and can be decomposed into two subproblems $f(x, \mu_c)$ and $g(k, \mu_c)$, which can be solved separately on the receiver and cell sides, respectively. In the following, we derive the solution to each of these subproblems.

USER SOLUTION

For the user solution given by $s(x, \mu_c)$, each user $k \in \mathcal{V}_{\mathcal{K}_c}$ is associated to the cell $c \in \mathcal{C}_T$ that maximizes

$$\begin{aligned} c^* = \arg\max &\left(\log(r^{[k,c]}) - \mu_c(t) \right) \\ \text{s.t.} &\sum_{c \in \mathcal{C}_T} x^{[k,c]} = 1, \ \forall k \in \mathcal{V}_{\mathcal{K}_c} \\ &x^{[k,c]} \in \{0, 1\}, \forall c \in \mathcal{C}_T, \forall k \in \mathcal{V}_{\mathcal{K}_c}, \end{aligned} \quad (44)$$

where t corresponds to the iteration of the gradient solution. Notice that, if there exist multiple cells satisfying (44), user k is assigned to one of them, and therefore, the number of users associated to each cell can be obtained as $K_{c^*} = \sum\limits_{k \in \mathcal{V}_{\mathcal{K}_c}} x^{[k,c^*]}$.

CELL SOLUTION

The maximum value of $g(k, \mu_c)$ is obtained solving

$$\frac{\partial g(K_c, \mu_c)}{\partial K_c} = 0 \Rightarrow K_c(t) = \exp(\mu_c - 1). \quad (45)$$

The Lagrangian multiplier can be defined as a message transmitted by the cell according to the number of users associated with it. Let us interpret K_{c^*} and K_c as the serving demand and serving supply for cell c, respectively. Thus, the multiplier μ_c is updated as

$$\mu_c(t+1) = \mu_c(t) - \delta(t) \cdot \left(K_c(t) - K_{c^*}(t) \right), \quad (46)$$

where $\delta(t)$ is a sufficiently step-size required for guaranteeing convergence. In (46), it can be seen that if cell c is overloaded, e.g., $K_{c^*} > K_c$, the multiplier μ_c increases, and therefore, less users are associated to this cell, otherwise the multiplier μ_c decreases in order to attract more users.

E. COMPLEXITY

For the centralized solution, the user assignment is obtained by exhaustively searching all of the possible connections between K_c users in each set $\mathcal{V}_{\mathcal{K}_c}$ and the available cells. Since, there are C optical cells and a single RF AP, the computational complexity of the centralized algorithm can be expressed as

$$\Theta \left(\prod_{k=1}^{K_c} (C+1) \right), \quad (47)$$

where Θ denotes the algorithm runtime complexity. For the centralized solution, the amount of information that must be exchanged is proportional to

$$((C+1)\times K_c)\,. \tag{48}$$

For the decentralized method, each of the $(C+1)$ cells, i.e., the C optical cells and the cell given by the RF system, transmits its multiplier μ_c, which comprises a relatively small number of bits, while each of the K_c users sends a connection request to a single cell. Hence, the amount of transmitted information among cells and users is proportional to

$$(C+1+K_c), \tag{49}$$

and the complexity of the decentralized algorithm is

$$\Theta\left((C+1)\times K_c\right). \tag{50}$$

The complexity required by the centralized approach increases exponentially with both the size of the network, i.e., cells and optical APs, and the number of users. However, the complexity increases linearly for the decentralized scheme. That is, the centralized solution requires a tremendous number of calculations for even a modest size network to reach the optimal solution. In contrast, the decentralized algorithm guarantees to converge to a near-optimal solution involving a much lower complexity. In this sense, in Section VI, it is shown that the solution provided by the decentralized approach is close to the optimal.

VI. SIMULATION RESULTS

We consider a 15 m × 15 m × 3 m indoor scenario where $L = 16$ optical APs are uniformly distributed on the ceiling of the room. The RF system is composed of a single WiFi AP. If it is not specified, $K = 20$ users are randomly distributed over the plane $h = 2.15$ m away from the ceiling. Each user is equipped with both a reconfigurable photodetector able to switch among $L = 16$ preset modes following an hemispherical arrangement and a RF transceiver. Similarly to [34], the costs of providing CSI are $\theta_{\text{fb}} = \theta_{\text{cd}} = 1\%$ and $\theta_{\text{ep}} = 4.76\%$. All other parameters of the considered VLC/WiFi network are listed in Table 1.

A. ACHIEVABLE RATE COMPARISON

The average user-rate of the cell formation approaches is shown in Fig. 9 considering $K = \{10, 20, 30, 40\}$ users randomly distributed in the room. It can be seen that the proposed dynamic cell formation provides greater user-rate than both static and full connectivity cell formation approaches for all the cases. Specifically, for $K = 10$, the average user-rate is equal to 43 Mbps. As expected, the user-rate decreases as the number of users grows since less network resources are allocated to each user. However, the improvement of the dynamic cell formation approach is greater for higher number of users. For instance, the user-rate is almost triple for dynamic cell formation in comparison with the full connectivity approach when $K = 40$. Therefore, we can conclude

TABLE 2. Simulation parameters.

VLC parameter	Value
Bandwidth for each LiFi AP	20 MHz
Physical area of the photodiode	15 mm^2
Transmitter semi-angle	45 deg
Receiver FOV	70 deg
Detector responsivity	0.53 A/W
Gain of optical filter	1.0
Cut-off frequency of optical channel	30 MHz
Wall-average reflectivity	0.63
Noise power spectral density	10^{-22}A^2/Hz
WiFi parameter	**Value**
OFDM subcarrier number	108
Transmitted power for Wi-Fi AP	20 dBm
Bandwidth for WiFi AP	40 MHz
Noise power of WiFi	-63 dBm

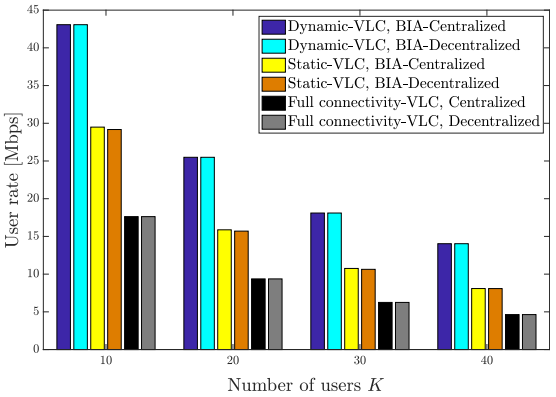

FIGURE 9. Achievable user-rate for distinct number of users after performing centralized and decentralized load balancing algorithms in the hybrid VLC/WiFi network.

that dynamic cell formation is a suitable grouping strategy for VLC systems. Furthermore, the decentralized load balancing algorithm provides a solution close, almost equal in most of cases, to the optimal given by the centralized algorithm with a much lower complexity. We focus exclusively on the decentralized algorithm from now on.

In Fig. 10, we plot the cumulative distribution function (CDF) of user-rate in comparison with some benchmark schemes. First, the dynamic cell formation jointly with the proposed load balancing algorithm provides a user-rate above 30 Mbps for most of the users. Besides, the 50$^{\text{th}}$ percentile corresponds to a sum-rate above 50 Mbps. For comparison purposes we consider that each optical cell transmits following the TPC scheme proposed in [8]. Interestingly, this approach obtains lower user-rate than the use of BIA for the proposed scheme. As discussed in [13], this fact is due to the constraints of the optical channel and the correlation among the channel responses of the users, which do not affect to BIA. Indeed, the correlation among preset modes of the same user is managed by the architecture of the reconfigurable photodetector. Furthermore, the use of BIA

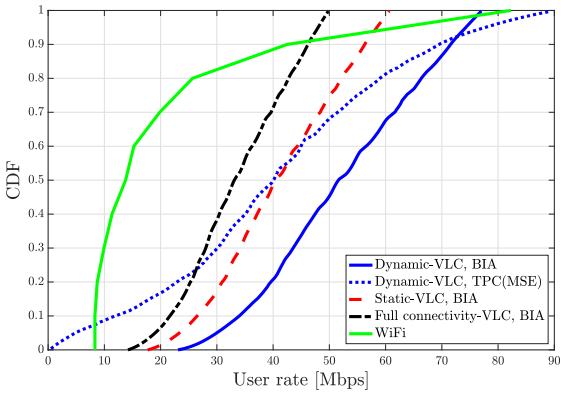

FIGURE 10. CDF of the user-rate in the VLC/RF hybrid network.

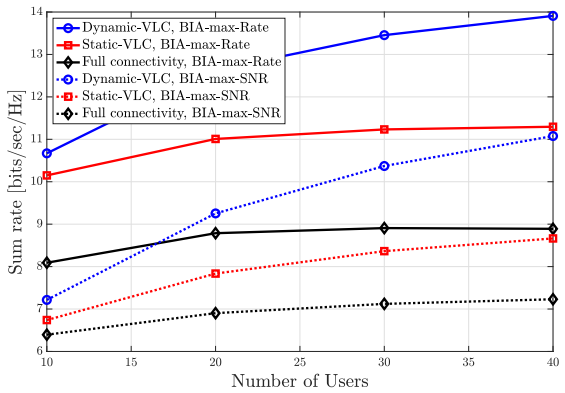

FIGURE 11. Average achievable sum-rate for the hybrid VLC/RF network.

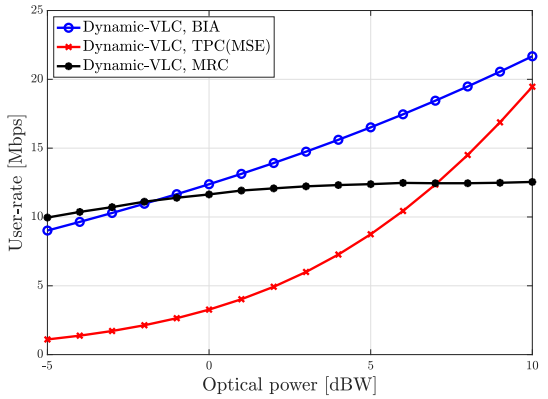

FIGURE 12. User-rate vs. transmitted optical power per optical AP in comparison with TPC and MRC.

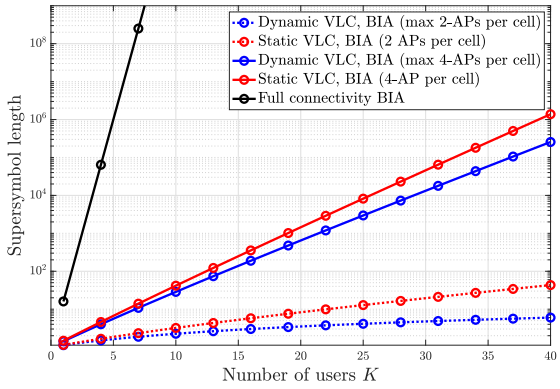

FIGURE 13. Comparison of the BIA supersymbol length for the proposed cell formation methodologies.

considering other cell formation methodologies penalyzes the user-rate considerably. It is interesting to remark that the full connectivity approach provides a poor user-rate due to the lack of effective connectivity. Moreover, the interference because of transmission to $K-1=19$ users is subtracted for this approach, which generates a great noise enhancement. The rate of the users connected to WiFi system is generally lower than the rate obtained by the users connected to VLC system. In this sense, the WiFi system can be interpreted as an umbrella network for blocked users in the VLC system and overloaded optical cells.

The achievable sum-rate considering different cell formation and user association schemes is plotted in Fig. 11 as the number of users increases. It can be easily seen that using the sum-rate as the variable to optimize improves the performance of the max-SNR strategies. It is worthy to remark that this improvement in sum-rate is given by the load balancing in the VLC/RF hybrid network. For instance, about 60% of the users are connected to WiFi system when considering a max-SNR association as is shown in Fig. 7, while this percentage is reduced considerably for the max-Rate approach as can be seen in Fig. 8. Besides, the proposed dynamic cell formation improves the achievable sum-rate in both max-SNR and max-Rate approaches with respect to both static and full connectivity cell formation methodologies.

In Fig. 12, we show the evolution of the user-rate achieved by the proposed schemes as the SNR increases in comparison with TPC based on MSE [8] and maximum ratio combining (MRC) [36] assuming the dynamic cell formation. First, notice that the proposed scheme based on BIA achieves greater user-rate than the other schemes in the considered SNR range. In comparison with TPC schemes, it can be seen that the slope of the user-rate is greater for high SNR values than for BIA, which results unsurprising since TPC schemes obtain higher multiplexing gain at the costs of providing CSIT. Therefore, high-SNR is required for TPC schemes to outperform the user-rate achieved by BIA. Furthermore, a comparison with MRC, which exploits the angular diversity of the reconfigurable photodetector, is carried out. It is shown that MRC obtains a good performance at low SNR. However, as the SNR increases MRC maintains an almost constant user-rate. We can conclude that the proposed scheme based on BIA results suitable for VLC in comparison with other schemes such as the considered above.

B. SUBERSYMBOL LENGTH

In Fig. 13, we plot the length of the resulting supersymbol for the considered cell formation methodologies. First, it is interesting to remark that the full connectivity approach generates extremely long supersymbols, which results unpractical in VLC networks where the coherence time is given by the users movement. For instance, considering only 8 users the supersymbol comprises $3.92\cdot10^9$ time slots for the full connectivity

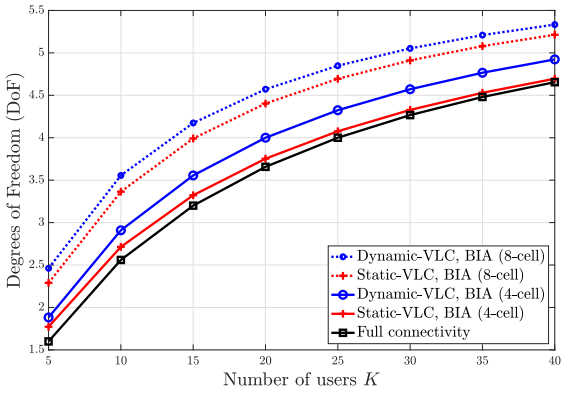

FIGURE 14. Achievable DoF for BIA based on the considered cell formation methodologies.

approach. In order to reduce the supersymbol length static cell formation based on creating optical cells with 2 and 4 optical APs each is analyzed. It can be seen that the supersymbol length decreases considerably as the VLC system is divided into smaller cells. For a fair comparison, dynamic cell formation is limited to the same number of optical APs per cell as for the static cell formation. Notice that there exists a slight difference in the length of the supersymbol between static and dynamic approaches, both considering the same number of cells. This is because the static cells are formed regardless of the user distribution, conversely the dynamic cells are formed and modified based on the distribution of users.

C. ACHIEVABLE DEGREES OF FREEDOM

Assuming BIA transmission in each optical cell, the sum-DoF provided by each of the considered cell formation methodologies is shown in Fig. 14. Again, the full connectivity approach provides less DoF than grouping the optical the APs in cells so that the users are only connected to the APs from which receive a useful signal. It can be also seen that dynamic cell formation achieves greater DoF than the static approach since it considers the distribution of users. For instance, assuming K equal to 10 users dynamic and static cell formation methodologies achieve 2.9 DoF and 2.5 DoF, respectively. Moreover, considering only 2 optical APs per cell, the achievable DoF slightly increase. However, the users may be subject to ICI. Therefore, there exists a trade-off between achievable DoF and ICI, which also determines the SNR degradation and the supersymbol length.

VII. CONCLUSION

In this work, we propose a dynamic cell formation method jointly with a load balancing strategy for hybrid VLC/RF networks. The proposed dynamic cell formation for VLC based on BIA provides greater DoF and user-rate than other approaches such as static cell formation or simply assuming full connectivity among all the optical APs to each user. Besides, this dynamic approach reduces the length of the BIA supersymbol in comparison with the baseline schemes, which relaxes the coherence time requirement. We devise a load balancing strategy taking into consideration the topology of the hybrid VLC/RF networks to manage the transmission resources. It is shown that maximizing the SNR does not correspond to maximizing the sum-rate since the distribution of the users may be unbalanced between the optical cells and the RF system. We propose both centralized and decentralized algorithms to optimize the resource allocation while managing the load balance of the hybrid network. Simulation results show that the proposed cell formation improves the performance in VLC/RF networks. Moreover, applying the devised load balancing algorithms, the proposed scheme achieves greater sum-rate than alternative schemes based on CSIT such as TPC for the same scenarios.

REFERENCES

[1] C.-X. Wang, F. Haider, X. Gao, X.-H. You, Y. Yang, D. Yuan, H. Aggoune, H. Haas, S. Fletcher, and E. Hepsaydir, "Cellular architecture and key technologies for 5G wireless communication networks," *IEEE Commun. Mag.*, vol. 52, no. 2, pp. 122–130, Feb. 2014.

[2] M. Z. Chowdhury, M. T. Hossan, A. Islam, and Y. M. Jang, "A comparative survey of optical wireless technologies: Architectures and applications," *IEEE Access*, vol. 6, pp. 9819–9840, 2018.

[3] L. Eduardo Mendes Matheus, A. Borges Vieira, L. F. M. Vieira, M. A. M. Vieira, and O. Gnawali, "Visible light communication: Concepts, applications and challenges," *IEEE Commun. Surveys Tuts.*, vol. 21, no. 4, pp. 3204–3237, 4th Quart., 2019.

[4] S. Al-Ahmadi, O. Maraqa, M. Uysal, and S. M. Sait, "Multi-user visible light communications: State-of-the-art and future directions," *IEEE Access*, vol. 6, pp. 70555–70571, 2018.

[5] V. R. Cadambe and S. A. Jafar, "Interference alignment and degrees of freedom of the K-user interference channel," *IEEE Trans. Inf. Theory*, vol. 54, no. 8, pp. 3425–3441, Aug. 2008.

[6] Q. H. Spencer, A. L. Swindlehurst, and M. Haardt, "Zero-forcing methods for downlink spatial multiplexing in multiuser MIMO channels," *IEEE Trans. Signal Process.*, vol. 52, no. 2, pp. 461–471, Feb. 2004.

[7] T. V. Pham, H. Le-Minh, and A. T. Pham, "Multi-user visible light communication broadcast channels with zero-forcing precoding," *IEEE Trans. Commun.*, vol. 65, no. 6, pp. 2509–2521, Jun. 2017.

[8] B. Li, J. Wang, R. Zhang, H. Shen, C. Zhao, and L. Hanzo, "Multiuser MISO transceiver design for indoor downlink visible light communication under per-LED optical power constraints," *IEEE Photon. J.*, vol. 7, no. 4, pp. 1–15, Aug. 2015.

[9] H. Marshoud, P. C. Sofotasios, S. Muhaidat, B. S. Sharif, and G. K. Karagiannidis, "Optical adaptive precoding for visible light communications," *IEEE Access*, vol. 6, pp. 22121–22130, 2018.

[10] S. A. Jafar, "Blind interference alignment," *IEEE J. Sel. Topics Signal Process.*, vol. 6, no. 3, pp. 216–227, Jun. 2012.

[11] T. Gou, C. Wang, and S. A. Jafar, "Aiming perfectly in the dark-blind interference alignment through staggered antenna switching," *IEEE Trans. Signal Process.*, vol. 59, no. 6, pp. 2734–2744, Jun. 2011.

[12] S. Begashaw, J. Chacko, N. Gulati, D. H. Nguyen, N. Kandasamy, and K. R. Dandekar, "Experimental evaluation of a reconfigurable antenna system for blind interference alignment," in *Proc. IEEE 17th Annu. Wireless Microw. Technol. Conf. (WAMICON)*, Apr. 2016, pp. 1–6.

[13] M. Morales-Cespedes, M. C. Paredes-Paredes, A. G. Armada, and L. Vandendorpe, "Aligning the light without channel state information for visible light communications," *IEEE J. Sel. Areas Commun.*, vol. 36, no. 1, pp. 91–105, Jan. 2018.

[14] M. Morales-Cespedes, A. A. Quidan, and A. G. Armada, "Experimental evaluation of the reconfigurable photodetector for blind interference alignment in visible light communications," in *Proc. 27th Eur. Signal Process. Conf. (EUSIPCO)*, Sep. 2019, pp. 1–5.

[15] Z. H. Abbas, F. Muhammad, and L. Jiao, "Analysis of load balancing and interference management in heterogeneous cellular networks," *IEEE Access*, vol. 5, pp. 14690–14705, 2017.

[16] I. Stefan, H. Burchardt, and H. Haas, "Area spectral efficiency performance comparison between VLC and RF femtocell networks," in *Proc. IEEE Int. Conf. Commun. (ICC)*, Jun. 2013, pp. 3825–3829.

[17] Y. Wang, X. Wu, and H. Haas, "Load balancing game with shadowing effect for indoor hybrid LiFi/RF networks," *IEEE Trans. Wireless Commun.*, vol. 16, no. 4, pp. 2366–2378, Apr. 2017.
[18] Y. Wang, D. A. Basnayaka, X. Wu, and H. Haas, "Optimization of load balancing in hybrid LiFi/RF networks," *IEEE Trans. Commun.*, vol. 65, no. 4, pp. 1708–1720, Apr. 2017.
[19] S. A. Jafar, "Topological interference management through index coding," *IEEE Trans. Inf. Theory*, vol. 60, no. 1, pp. 529–568, Jan. 2014.
[20] X. Li, F. Jin, R. Zhang, J. Wang, Z. Xu, and L. Hanzo, "Users first: User-centric cluster formation for interference-mitigation in visible-light networks," *IEEE Trans. Wireless Commun.*, vol. 15, no. 1, pp. 39–53, Jan. 2016.
[21] A. Adnan-Qidan, M. M. Cespedes, and A. G. Armada, "User-centric blind interference alignment design for visible light communications," *IEEE Access*, vol. 7, pp. 21220–21234, 2019.
[22] S. Corroy, L. Falconetti, and R. Mathar, "Dynamic cell association for downlink sum rate maximization in multi-cell heterogeneous networks," in *Proc. IEEE Int. Conf. Commun. (ICC)*, Jun. 2012, pp. 2457–2461.
[23] K. Son, S. Chong, and G. Veciana, "Dynamic association for load balancing and interference avoidance in multi-cell networks," *IEEE Trans. Wireless Commun.*, vol. 8, no. 7, pp. 3566–3576, Jul. 2009.
[24] H. Burchardt, S. Sinanovic, Z. Bharucha, and H. Haas, "Distributed and autonomous resource and power allocation for wireless networks," *IEEE Trans. Commun.*, vol. 61, no. 7, pp. 2758–2771, Jul. 2013.
[25] Q. Ye, B. Rong, Y. Chen, M. Al-Shalash, C. Caramanis, and J. G. Andrews, "User association for load balancing in heterogeneous cellular networks," *IEEE Trans. Wireless Commun.*, vol. 12, no. 6, pp. 2706–2716, Jun. 2013.
[26] X. Li, R. Zhang, and L. Hanzo, "Cooperative load balancing in hybrid visible light communications and WiFi," *IEEE Trans. Commun.*, vol. 63, no. 4, pp. 1319–1329, Apr. 2015.
[27] F. Jin, R. Zhang, and L. Hanzo, "Resource allocation under delay-guarantee constraints for heterogeneous visible-light and RF femtocell," *IEEE Trans. Wireless Commun.*, vol. 14, no. 2, pp. 1020–1034, Feb. 2015.
[28] J. M. Kahn and J. R. Barry, "Wireless infrared communications," *Proc. IEEE*, vol. 85, no. 2, pp. 265–298, Feb. 1997.
[29] V. Jungnickel, V. Pohl, S. Nonnig, and C. von Helmolt, "A physical model of the wireless infrared communication channel," *IEEE J. Sel. Areas Commun.*, vol. 20, no. 3, pp. 631–640, Apr. 2002.
[30] A. Nuwanpriya, S.-W. Ho, and C. S. Chen, "Indoor MIMO visible light communications: Novel angle diversity receivers for mobile users," *IEEE J. Sel. Areas Commun.*, vol. 33, no. 9, pp. 1780–1792, Sep. 2015.
[31] I. Ahmed, S. Orfali, T. Khattab, and A. Mohamed, "Characterization of the indoor-outdoor radio propagation channel at 2.4 GHz," in *Proc. IEEE GCC Conf. Exhib. (GCC)*, Feb. 2011, pp. 605–608.
[32] H.-S. Cha, S.-W. Jeon, and D. K. Kim, "Blind interference alignment for the K-user MISO BC under limited symbol extension," *IEEE Trans. Signal Process.*, vol. 66, no. 11, pp. 2861–2875, Jun. 2018.
[33] T. Gou, S. A. Jafar, and C. Wang, "On the degrees of freedom of finite state compound wireless networks," *IEEE Trans. Inf. Theory*, vol. 57, no. 6, pp. 3286–3308, Jun. 2011.
[34] S. A. Ramprashad, G. Caire, and H. C. Papadopoulos, "Cellular and network MIMO architectures: MU-MIMO spectral efficiency and costs of channel state information," in *Proc. Conf. Rec. 43rd Asilomar Conf. Signals, Syst. Comput.*, Nov. 2009, pp. 1811–1818.
[35] J. Mo and J. Walrand, "Fair end-to-end window-based congestion control," *IEEE/ACM Trans. Netw.*, vol. 8, no. 5, pp. 556–567, Oct. 2000.
[36] Z. Chen, D. A. Basnayaka, X. Wu, and H. Haas, "Interference mitigation for indoor optical attocell networks using an angle diversity receiver," *J. Lightw. Technol.*, vol. 36, no. 18, pp. 3866–3881, Sep. 15, 2018.

AHMAD ADNAN-QIDAN (Member, IEEE) received the B.Sc. degree in laser and optoelectronics engineering from AL-Nahrain University, Baghdad, Iraq, in 2012, and the M.Sc. degree in laser/electronic and communication engineering from the Institute of Laser for Postgraduate Studies, University of Baghdad, Baghdad, in 2015. He is currently pursuing the Ph.D. degree in multimedia and communications with the Universidad Carlos III de Madrid, Leganés, Spain. His research focus is on visible light communication, interference management, and hybrid networking.

MÁXIMO MORALES-CÉSPEDES (Member, IEEE) was born in Valdepeñas, Spain, in 1986. He received the B.Sc., M.Sc., and Ph.D. degrees from the Universidad Carlos III de Madrid, Spain, in 2010, 2012, and 2015, respectively, all in electrical engineering, with a specialization in multimedia and communications. From 2015 to 2017, he was working as a Postdoctoral Fellow of the Institute of Information and Communication Technologies, Electronics, and Applied Mathematics (ICTEAM), Universite Catholique de Louvain. He is currently with the Department of Signal Theory and Communications, Universidad Carlos III de Madrid. His research interests are in interference management, hardware implementations, MIMO techniques, and signal processing applied to wireless communications. In 2012, he was a Finalist of the IEEE Region 8 Student Paper Contest. He serves as an Editor for the IEEE COMMUNICATION LETTERS and has been a TPC Member of numerous IEEE conferences such as VTC, GLOBECOM, ICC, and WCNC.

ANA GARCÍA ARMADA (Senior Member, IEEE) received the Ph.D. degree in electrical engineering from the Polytechnical University of Madrid, in February 1998. She has been a Visiting Scholar with Stanford University, Bell Labs, and the University of Southampton. She is currently a Professor with the Universidad Carlos III de Madrid, Spain, where she is leading the Communications Research Group. She has coauthored eight book chapters on wireless communications and signal processing. She has published around 150 articles in international journals and conference proceedings, and she holds four patents. She has participated (coordinated most of them) in more than 30 national and 10 international research projects as well as 20 contracts with the industry, all of them related to wireless communications. Her main interests are multicarrier and multiantenna techniques, and signal processing applied to wireless communications. She has contributed to international standards organizations, such as ITU and ETSI, and is a member of the expert group of the European 5G PPP and the advisory committee 5JAC of the ESA, as an expert appointed by Spain on 5G. She has served on the TPC of more than 40 conferences, and she was a part of the organizing committee of the IEEE 5G Summit 2017, the IEEE Vehicular Technology Conference (VTC) Fall 2018, Spring 2018, and 2019, among others. She will be a part of the organizing committee of the IEEE GLOBECOM, in 2021 (general chair). She was the Secretary of the IEEE ComSoc Women in Communications Engineering Standing Committee, from 2016 to 2017, where she was the Chair, from 2018 to 2019. She was the Newsletter Editor of the IEEE ComSoc Signal Processing and Consumer Electronics Committee, from 2017 to 2018, where she has been the Secretary, since 2019. She has received the Young Researchers Excellence Award, the Award to Outstanding Achievement in Research, Teaching, and Management, and the Award to Best Practices in Teaching, all from the Universidad Carlos III de Madrid. She has received the Exemplary Editor Award, in 2017 and 2018. She was awarded the Third Place Bell Labs Prize 2014 for shaping the future of information and communications technology. She received the Outstanding Service Award from the IEEE ComSoc Signal Processing and Communications Electronics (SPCE) Technical Committee, in 2019. She has served on the Editorial Board of *Physical Communication*, from 2008 to 2017, and *IET Communications*, from 2014 to 2017. She has been serving on the Editorial Board of the IEEE COMMUNICATIONS LETTERS, since 2016 (an Editor, until February 2019, and a Senior Editor, since March 2019), and the IEEE TRANSACTIONS ON COMMUNICATIONS, since 2019.